

Electrodeposition mechanism of Ni–Al composite coating

Mohsen ADABI, Ahmad Ali AMADEH

School of Metallurgy and Materials Engineering, College of Engineering,
University of Tehran, P.O. Box 11155-4563, Tehran, Iran

Received 14 December 2013; accepted 16 April 2014

Abstract: Ni–Al composite coatings were electrodeposited from a modified Watts solution. The electrochemical behavior of the coatings was studied by means of zeta potential analysis, voltammetry and electrochemical impedance spectroscopy (EIS). It was found that the zeta potential of Al particles was -4 mV which is very close to that of Al_2O_3 . Moreover, addition of conductive Al particles into the electrolyte shifted the polarization curve to more negative potentials and loop size of EIS curve increased. It was also demonstrated that the co-deposition behavior of Ni–Al composite coatings obeys the Guglielmi's model. The results indicate that conductive Al particles behave as the inert particles and confirm the existence of a thin aluminum oxide layer on the surface of aluminum particles.

Key words: Ni–Al coating; zeta potential; voltammetry; electrochemical impedance spectroscopy (EIS)

1 Introduction

Composite coatings including a co-deposition of fine particles into a metal matrix are widely used in many applications such as aerospace and automotive industry. Among different methods used for fabrication of these coatings, electrodeposition is known as a simple and economic technique [1–4]. In recent years, many researches were carried out on Ni matrix coatings reinforced by ceramic particles, such as Ni– Al_2O_3 [5–7], Ni–SiC [8,9], Ni–WC [10], Ni– ZrO_2 [11], Ni– CeO_2 [12,13], Ni– TiO_2 [14] to improve their wear and corrosion resistance. However, little effort has been made on incorporation of metal particles into Ni matrix among them, composite Ni–Cr [15] and Ni–Al [16,17] coatings can be noted.

Study on polarization curves could give useful information about the mechanism of co-deposition of the particles into metal matrix, namely, addition of different particles, such as Al_2O_3 (non conductive particle), SiC (semi-conductive particle) and Cr (conductive particle) into the nickel electrolyte can affect the polarization curves and shift them to more negative or positive potentials. This displacement in reduction potential is attributed to an increase or decrease in the active surface area by the adsorbed particles on the cathode. In

co-deposition of nonconductive particles (Al_2O_3) [18,19], potential curve shifts to more negative values; whereas polarization curve shifts to more positive potential by addition of conductive Cr [15] and semi-conductive SiC [20,21] particles to the electrolyte. However, CUI et al [22] and ZHOU et al [23] observed a negative shift in polarization curve with addition of conductive Al particles to a given electrolyte for producing Ni/Cu–Al and Ni–Al, respectively. They suggested that a thin oxide layer might be present on the surface of Al particles, which changes the characteristics of Al particles and causes them to act similarly to inert particles during co-deposition [23]. Due to this similarity, incorporation of Al particles into a metal matrix should obey the Guglielmi's model established for co-deposition of inert particles [16,23]. Guglielmi's model takes place in two successive steps. In the first step, named loose adsorption, with physical nature, the particles are weakly absorbed on the cathode surface. In the second step, called strong adsorption, with electrochemical nature, the strong adsorption of particles occurs by reduction of enough amount of absorbed metal ions on the particles [24].

SUSAN et al [16], DAEMI et al [25] and BOSTANI et al [17] have produced Ni–Al composite coatings via conventional electrodeposition (CED) technique, in which the anode and cathode were vertically inserted in the bath. They indicated that the maximum values of

7% [16], 17% [25] and 25% [17] Al were incorporated into the coating in the presence of 225, 300, and 40 g/L of Al powder in electroplating bath, respectively. LIU and CHEN [26] and GHANBARI and MAHBOUBI [27] used a novel coating technique, called sediment co-deposition (SCD), to develop Ni–Al composite coating with the maximum values of 14% [26] and 22% [27] Al when adding 40 and 32 g/L Al particles to the electrolyte, respectively.

Most studies have been focused on the effect of process parameters (current density, stirring rate, etc.) as well as co-deposition mechanism of Ni–Al composite coatings by means of voltammetry and Guggenheim's model. To our knowledge, this mechanism has not been studied by electrochemical impedance spectroscopy (EIS). Hence, the present work deals with a more complete electrochemical study on incorporation of Al particles in Ni–Al composite coating produced by electrodeposition.

2 Experimental

Table 1 lists the composition of electrodeposition bath. The aluminum particles used were spherical and had a mean size of 3.5 μm , as shown in Fig. 1. To prevent the agglomeration of Al particles, the electrolytes containing different amounts of Al particles were premixed and stirred by a magnetic stirrer for 12 h and then by ultrasonic agitation for 30 min just prior to electrodeposition. The pH and temperature of the bath were fixed at 4 and 50 $^{\circ}\text{C}$, respectively. The Ni and Ni–Al coatings with 25 μm in thickness were prepared using square pulsed current with 50% duty cycle, 10 Hz frequency at various peak current densities. During electrodeposition, the bath was agitated by magnetic stirrer (250 r/min) to prevent the sedimentation of Al particles. Plates of 6061 aluminum alloys were used as cathode. The chemical composition of the alloy is given in Table 2. The plates with dimensions of 2 cm \times 3 cm \times 0.2 cm, were mechanically ground to 2000 grit SiC papers. The anode was a nickel plate with 99.9% purity. Prior to electroplating, aluminum substrates were first degreased in 50 g/L NaOH solution at 70 $^{\circ}\text{C}$ for 15 s. They were rinsed with distilled water and dipped in 65% (volume fraction) nitric acid solution for 5 s. They were then cleaned with distilled water and dipped in a zincate bath (30 g/L Ni(SO₄)₂, 40 g/L ZnSO₄, 106 g/L NaOH, 10 g/L KCN, 40 g/L KHC₄H₄O₆, 5 g/L CuSO₄ and 2 g/L FeCl₂). Finally, the specimens were dipped in the

Table 1 Composition of electroplating bath (g/L)

Nickel sulfate (NiSO ₄ ·6H ₂ O)	Nickel chloride (NiCl ₂ ·6H ₂ O)	Boric acid (H ₃ BO ₃)	Sodium dodecyl sulphate	Aluminum particles
300	45	45	0.25	up to 50 g/L

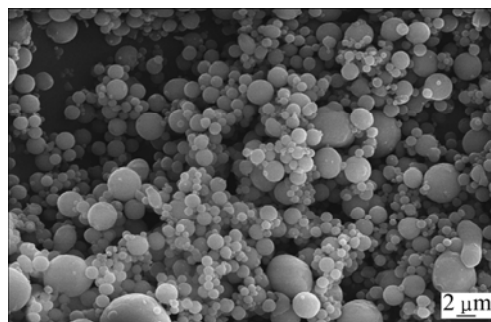


Fig. 1 SEM image of as-received Al particles

Table 2 Composition of 6061 aluminum alloy used in this work (mass fraction, %)

Si	Fe	Cu	Mn	Mg
0.36	0.2	0.01	0.02	0.52
Cr	Zn	Ti	Al	
0.03	0.01	0.02	Bal.	

electrolyte for electrodeposition process.

The surface morphology and elemental analysis of the samples were studied using a VegaTescan scanning electron microscope (SEM) equipped with energy dispersive X-ray spectrometer (EDS). Phase analysis of the coating was carried out by X-ray diffraction (XRD) using Philips Xpert pro type with Cu K α radiation at a voltage of 20 kV.

The zeta potential of Al particles was determined at pH of 4 by zeta potential analyzer instrument (zeta plus). All measurements were performed at least triple times, at room temperature. The voltammetry tests were carried out to understand the particles–cathode interactions by an EG&G potentiostat model 273A at a scan rate of 10 mV/s. Electrochemical impedance spectra of the process were acquired in the frequency range from 100 kHz to 5 mHz, with a signal amplitude of 10 mV.

3 Results and discussion

3.1 Morphological characteristics

Backscattered and secondary electrons images of Ni–Al composite coating deposited from the bath containing 50 g/L Al particles at 2 A/dm² are shown in Figs. 2(a) and (b), respectively. Dark spherical Al particles characterized by EDS analysis (Fig. 2(c)) are homogeneously distributed in white nickel matrix (Fig. 2(a)). Some holes, the trace of Al particles pulled out from Ni matrix, can also be observed in Fig. 2(b). EDS analysis (Fig. 2(d)) displays the presence of 15% Al in this composite coating, which is more than the value reported by LIU and CHEN [26] and GHANBARI and MAHBOUBI [27] at the same current density. This difference may be due to using of pulse current in our

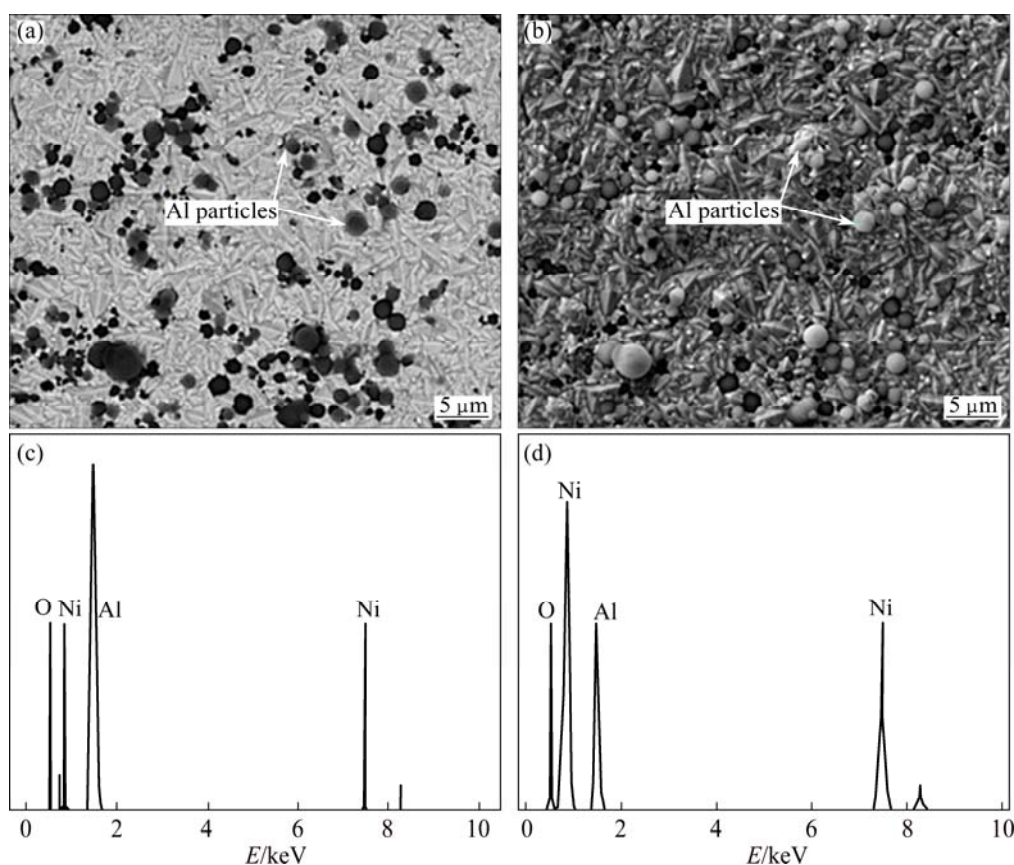


Fig. 2 BSE (a) and SE (b) images of Ni–Al composite coating, EDS analysis (c) of dark points shown in (a), typical EDS analysis (d) of Ni–Al composite coating

experiments, whereas they applied direct current. It was reported that incorporation of particles into the matrix in pulse electrodeposition is more than that in direct one [28].

X-ray diffraction (XRD) patterns of the samples electroplated for the electrolytes without Al and with 50 g/L Al are shown in Fig. 3. The patterns show typical peaks corresponding to (111) and (200) crystallographic planes of nickel. For pure nickel, (200) is the preferred orientation of this coating. Apparently, [100] is the preferred grain growth direction for face centered cubic crystals [29]. As indicated in this figure, the intensity of (111) peak in the XRD pattern increases with addition of Al particles (Fig. 3(b)), namely, the incorporation of Al particles into the coating suppresses (200) preferred growth and consolidates the (111) orientation.

3.2 Surface properties of Al particles

Zeta potential of Al particles in electroplating bath at pH 4 is shown in Table 3. Zeta potential is defined as the electrical potential at the interface of solid particle and electrolyte. It is related to the surface charge of the particle, adsorbed interface layers, and the composition of the electrolyte. As shown in Table 3, zeta potential decreases in the presence of SDS surfactant. SDS is an

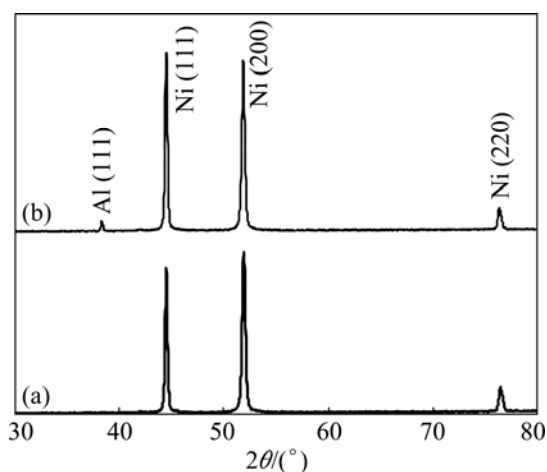


Fig. 3 XRD pattern of pure Ni (a) and Ni–Al composite coatings (b)

Table 3 Zeta potential of Al particles at pH 4 with or without SDS surfactant

Type of particles in Watts bath	Zeta potential/mV
Al	–4
Al with 0.25 g/L SDS	–47
Al ₂ O ₃	–4.5 [30]

anionic surfactant that one of its ends is hydrophobic and the other is hydrophilic. The SDS molecules are adsorbed on Al particles with their hydrophobic part and their negative part turning towards the electrolyte, so the negative surface charge of the particle increases. Besides, it was found that zeta potential of Al particles is very close to that of Al_2O_3 reported by CHEN et al [30]. It may be due to the coverage of Al particles with a very thin amorphous Al_2O_3 layer [31–33]. Hence, Al particles can act as inert particles during co-deposition. For better clarification of the effect of Al particles during co-deposition, more investigations were carried out and the results are presented in the following sections.

3.3 Potentiodynamic polarization

Figure 4 presents the potentiodynamic polarization curves at 10 mV/s potential sweep rate. The potential was swept in the cathodic direction from -0.2 to -1.2 V versus Ag/AgCl. It is seen that the addition of Al particles to the electrolyte shifts the reduction potential of nickel towards more negative. This shift to lower potentials is enhanced by increasing the amount of Al particles in the bath. Such behavior was also observed for Ni [23] and Ni/Cu [22] electrolytes after addition of Al particles. The negative shift is attributed to a decrease in the active surface area of the cathode due to the adsorption of Al particulates and this is characteristics of co-deposition of inert particles with nickel ions. In fact, it is believed that existence of a thin aluminum oxide in its amorphous form [31–33] on the surface of Al particles can change their surface properties during co-deposition.

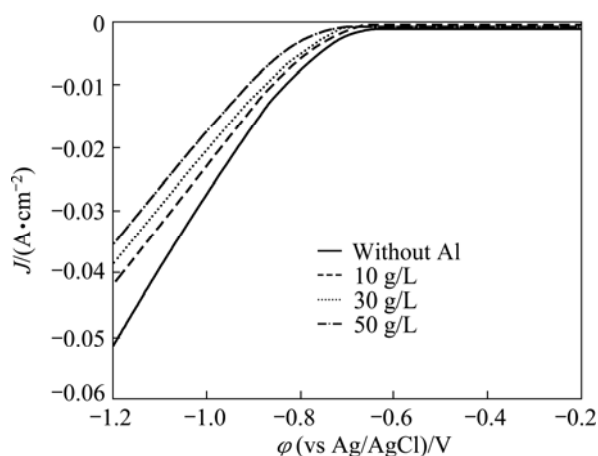


Fig. 4 Cathodic polarization curves of Ni deposition in bath containing different concentrations of Al particles

3.4 EIS studies

The Nyquist plots of electrochemical impedance spectroscopy for Ni and Ni–Al coatings are shown in Fig. 5. The impedance comprises a high frequency capacitive loop followed by a low frequency inductive loop. The loop size is found to increase with increasing

the concentration of Al particles in the bath. For better understanding of the effect of Al incorporation on nickel electrodeposition, the mechanisms suggested for pure nickel should be considered.

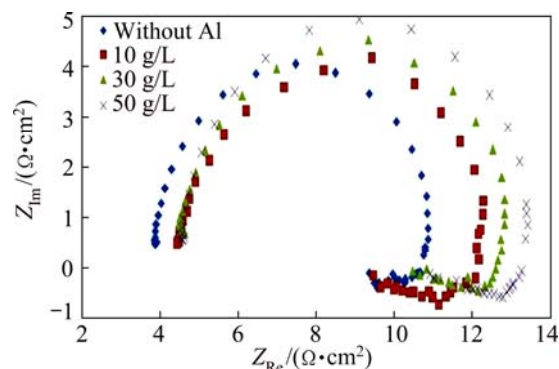
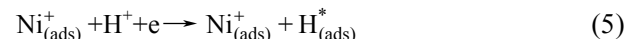
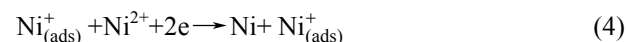
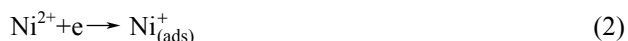


Fig. 5 EIS Nyquist plots of samples electrodeposited in electrolyte without Al (a) and with 10 g/L (b), 30 g/L (c) and 50 g/L (d) at potential of -750 mV (vs Ag/AgCl) with 10 mV amplitude and frequency range between 5 mHz and 100 kHz

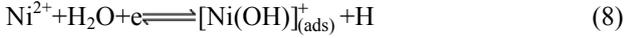
The mechanism of Ni electrodeposition from acidic solutions (chloride, sulphate and Watts) has been extensively studied by EPELBOIN and WIART [34]. There are usually two semicircles in the Nyquist plots. The capacitive loop at high frequencies represents the double layer capacitance and inductive loop at low frequencies is related to interactions between nickel and hydrogen discharge. It was suggested that $\text{Ni}_{(\text{ads})}^+$ behaves as an intermediate for nickel electrodeposition as well as a catalyst for forming $\text{H}_{(\text{ads})}^*$ species. It was considered that the hydrogen evolution was inhibited by $\text{H}_{(\text{ads})}^*$. Consequently, the active area is closely connected to the extent of coverage by these species [35–37].

Further impedance studies showed that Ni electrodeposition occurs through different elementary steps depending on the pH. The following mechanism was suggested by EPELBOIN and WIART [34] for $\text{pH} \leq 3$:



In Epelboin mechanism ($\text{pH} \leq 3$), the $\text{Ni}_{(\text{ads})}^+$ species predominates on the electrode surface whereas according to SANTANA et al [38], Ni electrodeposition at pH 4–6 involves two different values species:

$[\text{Ni}(\text{OH})]_{\text{ads}}^+$ and $[\text{Ni}(\text{OH})]_{\text{ads}}$. At these pH values, $\text{Ni}_{(\text{ads})}^+$ species should have OH^- in its composition. The suggested mechanism is



As mentioned above, the inductive loop in Nyquist plot of pure nickel electrodeposition is related to the adsorption of intermediate species such as $[\text{Ni}(\text{OH})]_{(\text{ads})}^+$ and $\text{Ni}_{(\text{ads})}^+$. Addition of Al particles into the solution may affect the intermediate reactions. The same results were reported for co-deposition of Ni–SiC. It was proposed that the reduction paths of $\text{Ni}_{(\text{ads})}^+$ change when the electrolyte contains SiC particles [39,40].

The equivalent circuit used to explain the electrodeposition process of Ni and Ni–Al coatings is presented in Fig. 6. In this circuit, R_s represents the solution resistance between the reference and working electrodes; R_{ct} is the charge transfer resistance; C_{dl} is the double layer capacitance and the parallel connection of a resistor (R_{ads}) with an inductor (L_{ads}) represents the existence of an adsorption process. These parameters calculated for Ni and Ni–Al (the concentration of Al particles in the bath was 50 g/L) coatings by means of fitting procedure are shown in Table 4. Addition of Al particles into the solution increases the charge transfer resistance which causes in-activating the nickel reduction; whereas BENEVA et al [41] observed the opposite tendency with adding SiC particles.

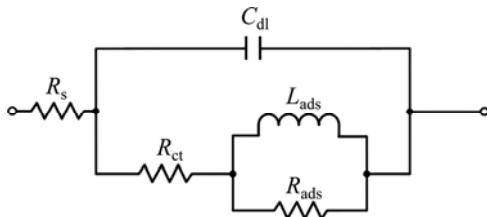


Fig. 6 Equivalent electrical circuit of Ni and Ni–Al deposition system

Table 4 Impedance parameters in Ni and Ni–Al (Al particles concentration in bath was 50 g/L) deposition system

Coating	R_s/Ω	R_{ct}/Ω	R_{ads}/Ω	$C_{\text{dl}}/\mu\text{F}$	L_{ads}/H
Pure Ni	3.9	5.5	2.2	1036	0.09
Ni–Al composite	4.5	6.5	3.5	750	0.1

3.5 Co-deposition mechanism

Among different models presented for co-deposition mechanism of solid particles into a metal matrix,

Guglielmi's model is the most accepted one. It has also been examined with different co-deposition systems such as Ni–SiC and Ni–TiO₂ [24].

The mathematical equations deduced by Guglielmi model [24] are

$$\frac{\alpha}{1-\alpha} = \frac{nFd\nu_0}{Wi_0} \exp[(A-B)\eta] \cdot \frac{kC}{1+kC} \quad (12)$$

$$J = (1-\theta)J_0e^{A\eta} \quad (13)$$

where α is the volume fraction of particles in the coating; C is the volume fraction of particles in the plating bath; W is the relative atomic mass of deposited metal; n is the valence of deposited metal; F is the Faraday's constant; d is the density of deposited metal; ν_0 is constant for particle deposition; A and B are constant for metal deposition and particle deposition; k is adsorption coefficient; J_0 is exchange current density of deposited metal; η and J are overpotential and current density, respectively; θ is surface coverage of embedded particles.

In the restricted case of low values of α , the terms $(1-\alpha)$ and $(1-\theta)$ can be omitted. However, in the present Ni–Al system, α value is such high that factors of $(1-\alpha)$ and $(1-\theta)$ cannot be dropped.

Substituting Eq. (13) into Eq. (12), it is obtained

$$\frac{C(1-\alpha)^{(2-B/A)}}{\alpha} = \frac{WJ_0^A}{nFd\nu_0} \cdot J^{(1-B/A)} \cdot \left(\frac{1}{k} + C\right) \quad (14)$$

Plotting the $C(1-\alpha)^{(2-B/A)}/\alpha$ against C for various current densities results in a sheaf of straight lines having the common intersection on the point $-1/k$ with the C -axis. The slope of these lines is

$$\tan \varphi = \frac{WJ_0^A}{nFd\nu_0} \cdot J^{(1-B/A)} \quad (15)$$

Taking logarithms, a linear relationship between $\lg(\tan \varphi)$ and $\lg J$ will be obtained.

$$\lg(\tan \varphi) = \lg \frac{WJ_0^A}{nFd\nu_0} + \left(1 - \frac{B}{A}\right) \lg J \quad (16)$$

The slope of this line is equal to $(1-B/A)$.

The B/A ratio should be pre-determined for fitting the experimental data in Eq. (14). This ratio is obtained in following way.

For coatings produced with different current densities, the plot of $C(1-\alpha)^{(2-B/A)}/\alpha$ against C presents a series of straight lines. The selected B/A ratio must converge these lines towards the same point on the C -axis (i.e. $C=-1/k$).

The logarithm of slopes of lines ($\lg(\tan \varphi)$) obtained from the graph of $C(1-\alpha)^{(2-B/A)}/\alpha$ vs C plotted against $\lg J$,

($\lg(\tan \varphi)$ vs $\lg J$), lies on a straight line. According to Eq. (16), the slope of this line is equal to $(1-B/A)$. The obtained B/A ratio should be equal to the selected one.

In Fig. 7(a) the experimental results, considering the B/A ratio equal to 0.24, have been presented. It is clear that experimental data can be well fitted on a sheaf of straight lines converging at a negative point on the C -axis. From extrapolation of these lines, the $-1/k$ point of intersection with C -axis is equal to -0.62 . In Fig. 7(b), the logarithm of the slopes of the straight lines in Fig. 7(a) ($\lg(\tan \varphi)$) is plotted vs $\lg J$. The slope of this line is 0.76 and so the B/A ratio is 0.24. This value is exactly equal to the B/A value considered previously for initial curve fitting. Hence, the co-deposition behavior of Ni–Al system is in good agreement with the Guglielmi's model [24].

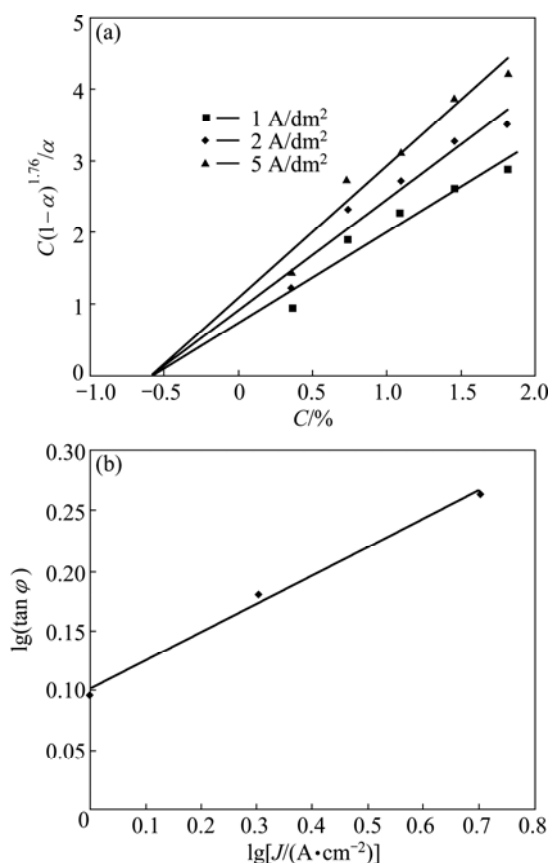


Fig. 7 Curves of $C(1-\alpha)^{1.76}/\alpha$ vs C for Ni–Al coatings in various current densities (a) and $\lg(\tan \varphi)$ vs $\lg J$ for Ni–Al coatings (b)

4 Conclusions

1) Zeta potential of Al is similar to that of Al_2O_3 particles.

2) Addition of Al particles shifts the reduction potential of Ni to more negative values. The displacement in reduction potential is attributed to a decrease in the active surface area.

3) The loop size of EIS curves increases with adding Al particles to Ni electrolyte. It can be due to an increase in charge transfer resistance.

4) The co-deposition behavior of Ni–Al composite coatings obeys the Guglielmi's model.

5) The results are similar to the co-deposition of inert particles (e.g. Al_2O_3) in metal matrix and confirm the existence of a thin aluminum oxide layer on the surface of aluminum particles.

References

- [1] ABDEL A. Hard and corrosion resistant nanocomposite coating for Al alloy [J]. *Materials Science and Engineering A*, 2008, 474(1–2): 181–187.
- [2] ARUNA S T, WILLIAM GRIPS V K, RAJAM K S. Ni-based electrodeposited composite coating exhibiting improved microhardness, corrosion and wear resistance properties [J]. *Journal of Alloys and Compounds*, 2009, 468(1–2): 546–552.
- [3] SHRESTHA N K, SAKURADA K, MASUKO M, SAJI T. Composite coatings of nickel and ceramic particles prepared in two steps [J]. *Surface and Coatings Technology*, 2001, 140(2): 175–181.
- [4] MEDLIENE V. The influence of B_4C and SiC additions on the morphological, physical, chemical and corrosion properties of Ni coatings [J]. *Surface and Coatings Technology*, 2002, 154(1): 104–111.
- [5] CHEN L, WANG L, ZENG Z, XU T. Influence of pulse frequency on the microstructure and wear resistance of electrodeposited Ni– Al_2O_3 composite coatings [J]. *Surface and Coatings Technology*, 2006, 201(3–4): 599–605.
- [6] SZCYGIEL B, KOLODZIEJ M. Composite Ni/ Al_2O_3 coatings and their corrosion resistance [J]. *Electrochimica Acta*, 2005, 50(20): 4188–4195.
- [7] GUL H, KILIC F, ASLAN S, ALP A, AKBULUT H. Characteristics of electro-co-deposited Ni– Al_2O_3 nano-particle reinforced metal matrix composite (MMC) coatings [J]. *Wear*, 2009, 267(5–8): 976–990.
- [8] GER M D. Electrochemical deposition of nickel/ SiC composites in the presence of surfactants [J]. *Materials Chemistry and Physics*, 2004, 87(1): 67–74.
- [9] NOWAK P, SOCHAR P, KAISHEVA M, FRANSAER J, CELIS J P, STOINNOV Z. Electrochemical investigation of the codeposition of SiC and SiO_2 particles with nickel [J]. *Journal of Applied Electrochemistry*, 2000, 30(40): 429–437.
- [10] SURENDER M, BASU B, BALASUBRAMANIAM R. Wear characterization of electrodeposited Ni–WC composite coatings [J]. *Tribology International*, 2004, 37(9): 743–749.
- [11] WANG W, HOU F Y, WANG H, GUO H T. Fabrication and characterization of Ni– ZrO_2 composite nano-coatings by pulse electrodeposition [J]. *Scripta Materialia*, 2005, 53(5): 613–618.
- [12] QU N S, ZHU D, CHAN K C. Fabrication of Ni– CeO_2 nanocomposite by electrodeposition [J]. *Scripta Materialia*, 2006, 54(7): 1421–1425.
- [13] XUE Y J, JIA X Z, ZHOU Y W, MA W, LI J S. Tribological performance of Ni– CeO_2 composite coatings by electrodeposition [J]. *Surface and Coatings Technology*, 2006, 200(20–21): 5677–5681.
- [14] LAJEVARDI S A, SHAHRABI T. Effects of pulse electrodeposition parameters on the properties of Ni–TiO₂ nanocomposite coatings [J]. *Applied Surface Science*, 2010, 256(22): 6775–6781.
- [15] WATSON S W, WALTERS R P. The effect of chromium particles on nickel electrodeposition [J]. *Journal of the Electrochemical Society*, 1991, 138(12): 3633–3637.

- [16] SUSAN D F, BARMAK K, MARDER A R. Electrodeposited Ni–Al particle composite coatings [J]. *Thin Solid Films*, 1997, 307(1–2): 133–140.
- [17] BOSTANI B, ARGHAVANIAN R, PARVINI-AHMADI N. Study on particle distribution, microstructure and corrosion behavior of Ni–Al composite coatings [J]. *Materials and Corrosion*, 2012, 63(4): 323–327.
- [18] WEBB P R, ROBERTSON N L. Electrolytic codeposition of Ni– γ -Al₂O₃ thin films [J]. *Journal of the Electrochemical Society*, 1994, 141(3): 669–673.
- [19] MORALES A L, PODLAHA E J. The effect of Al₂O₃ nanopowder on Cu electrodeposition [J]. *Journal of the Electrochemical Society*, 2004, 151(7): C478–C483.
- [20] WATSON S W. Electrochemical study of SiC particle occlusion during nickel electrodeposition [J]. *Journal of the Electrochemical Society*, 1993, 140(8): 2235–2238.
- [21] BAHADRMANESH B, DOLATI A, AHMADI M R. Electrodeposition and characterization of Ni–Co/SiC nanocomposite coatings [J]. *Journal of Alloys and Compounds*, 2011, 509(39): 9406–9412.
- [22] CUI X, WEI W, LIU H, CHEN W. Electrochemical study of codeposition of Al particle-nanocrystalline Ni/Cu composite coatings [J]. *Electrochimica Acta*, 2008, 54(2): 415–420.
- [23] ZHOU Y B, QIAN B Y, ZHANG H J. Al particles size effect on the microstructure of the co-deposited Ni–Al composite coatings [J]. *Thin Solid Films*, 2009, 517(11): 3287–3291.
- [24] GUGLIELMI N. Kinetics of the deposition of inert particles from electrolytic baths [J]. *Journal of the Electrochemical Society*, 1972, 119(8): 1009–1012.
- [25] DAEMI N, MAHBOUBI F, ALIMADADI H. Effect of plasma nitriding on electrodeposited Ni–Al composite coating [J]. *Materials and Design*, 2011, 32(2): 971–975.
- [26] LIU H, CHEN W. Electrodeposited Ni–Al composite coating with high Al content by sediment co-deposition [J]. *Surface and Coatings Technology*, 2005, 191(2–3): 341–350.
- [27] GHANBARI S, MAHBOUBI F. Corrosion resistance of electrodeposited Ni–Al composite coatings on the aluminum substrate [J]. *Materials and Design*, 2011, 32(4): 1859–1864.
- [28] HOU K H, HWU W H, KE S T, GER M D. Ni–P–SiC composite produced by pulse and direct current plating [J]. *Materials Chemistry and Physics*, 2006, 100(1): 54–59.
- [29] BOKAR T, HARIMKAR S P. Effect of electrodeposition conditions and reinforcement content on microstructure and tribological properties of nickel composite coatings [J]. *Surface and Coatings Technology*, 2011, 205(17–18): 4124–4134.
- [30] CHEN L, WANG L, ZENG Z, ZHANG J. Effect of surfactant on the electrodeposition and wear resistance of Ni–Al₂O₃ composite coatings [J]. *Materials Science and Engineering A*, 2006, 434(1–2): 319–325.
- [31] LUO P, NIEH T G, SCHWARTZ A J, LENK T J. Surface characterization of nanostructured metal and ceramic particles [J]. *Materials Science and Engineering A*, 1995, 204(1–2): 59–64.
- [32] CHAMPION Y, BIGO J. Synthesis and structural of aluminium nanocrystalline [J]. *NanoStructured Materials*, 1998, 10(7): 1097–1100.
- [33] PHUNG X Y, GROZA J, STACH E A. Surface characterization of metal nanoparticles [J]. *Materials Science and Engineering A*, 2003, 359(1): 261–268.
- [34] EPELBOIN I, WIART R. Mechanism of the electrocrystallization of nickel and cobalt in acidic solution [J]. *Journal of the Electrochemical Society*, 1971, 118(10): 1577–1582.
- [35] EPELBOIN I, JOUSSELIN M, WIART R. Impedance measurement for nickel deposition in sulfate and chloride electrolytes [J]. *Journal of Electroanalytical Chemistry*, 1981, 119(1): 61–71.
- [36] EPELBOIN I, JOUSSELIN M, WIART R. Impedance of nickel deposition from sulfate and chloride electrolytes [J]. *Journal of Electroanalytical Chemistry*, 1979, 101(2): 281–284.
- [37] MATULIS J, SILZYS R. On some characteristics of cathodic processes in nickel electrodeposition [J]. *Electrochimica Acta*, 1964, 9(9): 1177–1188.
- [38] SANTANA A I C, DIAZ S L, BARCIA O E, MATTOS O R. A kinetic study on nickel electrodeposition from sulfate acid solutions [J]. *Journal of Electroanalytical Chemistry*, 2009, 156(8): 326–330.
- [39] YE H S, WAN C C. Codeposition of SiC powders with nickel in a Watts bath [J]. *Journal of Applied Electrochemistry*, 1994, 24(10): 993–1000.
- [40] HU F, CHAN K C. Deposition behaviour and morphology of Ni–SiC electro-composites under triangular waveform [J]. *Applied Surface Science*, 2005, 243(1–4): 251–258.
- [41] BENE L, BONORA P L, BORELLO A, MARTELLI S, WENGER F, PONTTHIAUXE P, GALLAND J. Preparation and investigation of nanostructured SiC–nickel layers by electrodeposition [J]. *Solid State Ionics*, 2002, 151(1–4): 89–95.

镍–铝复合涂层的电沉积机理

Mohsen ADABI, Ahmad Ali AMADEH

College of Engineering, School of Metallurgy and Materials Engineering,
University of Tehran, P.O. Box 11155-4563, Tehran, Iran

摘要: 在改进的 Watts 溶液中电沉积镍–铝复合涂层。采用 Z 电位分析、伏安法和电化学阻抗谱(EIS), 研究涂层的电化学行为。结果发现, 铝颗粒的 Z 电位是–4 mV, 与氧化铝的非常接近。添加导电铝颗粒到电解液中, 导致极化曲线向负电位方向移动, 且 EIS 曲线的环路尺寸增大。结果表明, 镍–铝复合层的共沉积行为服从 Guglielmi 模型。加入的导电铝颗粒起惰性粒子的作用, 证实在铝颗粒表面存在薄的氧化铝层。

关键词: 镍–铝涂层; Z 电位; 伏安法; 电化学阻抗谱

(Edited by Xiang-qun LI)